Experimental Test of the Quantum No-Hiding Theorem

Jharana Rani Samal,[1,*] Arun K. Pati,[2] and Anil Kumar[1]

[1]Department of Physics and NMR Research Centre, Indian Institute of Science, Bangalore, India
[2]Harish-Chandra Research Institute, Chhatnag Road, Jhunsi, Allahabad 211 019, India

(Received 9 September 2010; published 22 February 2011)

The no-hiding theorem says that if any physical process leads to bleaching of quantum information from the original system, then it must reside in the rest of the Universe with no information being hidden in the correlation between these two subsystems. Here, we report an experimental test of the no-hiding theorem with the technique of nuclear magnetic resonance. We use the quantum state randomization of a qubit as one example of the bleaching process and show that the missing information can be fully recovered up to local unitary transformations in the ancilla qubits.

DOI: 10.1103/PhysRevLett.106.080401 PACS numbers: 03.65.Ta, 03.65.Wj, 03.67.−a, 76.60.−k

Linearity and unitarity are two fundamental tenets of quantum theory. Any consequence that follows from these must be respected in the quantum world. The no-cloning [1] and the no-deleting theorems [2] are the consequences of the linearity and the unitarity. Together with the stronger no-cloning theorem they provide permanence to quantum information [3], thus suggesting that in the quantum world information can be neither created nor destroyed. This is also connected to conservation of quantum information [4]. In this sense quantum information is robust, but at the same time it is also fragile because any interaction with the environment may lead to loss of information. The no-hiding theorem [5] addresses precisely the issue of information loss.

There are many physical processes in nature where one can apply the no-hiding theorem. The examples can be cited starting from quantum teleportation [6], state randomization and thermalization [7], private quantum channels [8], to black hole evaporation [9]. If the original information about the system has disappeared, then one may wonder where it has gone. The no-hiding theorem proves that if the information is missing from one system then it simply goes and remains in the rest of the Universe. The missing information cannot be hidden in the correlations between the system and the environment [5].

Consider a physical process which transforms an arbitrary pure state $\rho = |\psi\rangle\langle\psi|$ to a fixed mixed state σ that has no dependence on the input state. Let $\sigma = \sum_k p_k |k\rangle\langle k|$, where the p_k are the nonzero eigenvalues with $\sum_k p_k = 1$ and $|k\rangle$ are the eigenvectors. This process can be thought of as a generalization of the Landauer erasure [10]. Now, the bleaching process can be expressed in terms of the Schmidt decomposition of the final state as $|\psi\rangle \to |\Psi\rangle = \sum_{k=1}^{K} \sqrt{p_k}\,|k\rangle \otimes |A_k(\psi)\rangle$, where $\mathrm{Tr}_A(|\Psi\rangle\langle\Psi|) = \sigma$ and $\{|A_k\rangle\}$ are the orthonormal states of the ancilla. Using the linearity and the unitarity of quantum mechanics one can show that the final state must be of the following form [5],

$$|\Psi\rangle = \sum_{k=1}^{K} \sqrt{p_k}\,|k\rangle \otimes (|q_k\rangle \otimes |\psi\rangle \oplus 0), \tag{1}$$

where $\{|q_k\rangle\}$ is an orthonormal set of K states and $\oplus 0$ denotes the fact that we substitute any unused dimensions of the ancilla space by zero vectors. This shows that the missing information about $|\psi\rangle$ can be found entirely within the ancilla and no information is hidden in the bipartite correlations of the system and the ancilla.

The simplest example of a bleaching process is the quantum state randomization where an arbitrary pure state in a d-dimensional Hilbert space transforms to a completely mixed state, i.e., $|\psi\rangle\langle\psi| \to \frac{I}{d}$. For any arbitrary qubit the state randomization is a completely positive map as given by $|\psi\rangle\langle\psi| \to \frac{1}{4}\sum_{k=0}^{3} \sigma_k |\psi\rangle\langle\psi|\sigma_k = \frac{I}{2}$, where $\sigma_0 = I$ and σ_k $(k = 1, 2, 3)$ are the Pauli matrices. The above map can be thought of as a unitary map by attaching two qubits as the ancilla which is given by

$$|\psi\rangle|A\rangle \to |\Psi\rangle = \frac{1}{2}\sum_{k=0}^{3} \sigma_k |\psi\rangle|A_k\rangle, \tag{2}$$

where $|A_k\rangle$ are orthonormal and the initial state of the ancilla is $|A\rangle = \frac{1}{2}\sum_{k=0}^{3}|A_k\rangle = \frac{1}{2}(|00\rangle + |01\rangle + |10\rangle + |11\rangle)$. The unitary operator that realizes the above randomization operation is a conditional unitary operator given by $U = \sum_{k=0}^{3} \sigma_k \otimes |A_k\rangle\langle A_k|$. We can see that if we trace out the ancilla qubits from the final state given in (2), we do get a completely mixed state. Now, the important question is, where has the missing information gone that has bleached out from the original qubit? The no-hiding theorem provides an answer to this question.

In the above example, we will see that the missing information is simply residing in the two qubit ancilla state. This is the essence of the no-hiding theorem. To reconstruct the original state $|\psi\rangle$ from the ancilla qubits, we need to apply the ancilla local unitary $U_{23} = \mathrm{CNOT}_{23}(H_2 \otimes I_3)\mathrm{CNOT}_{23}$ (Fig. 1). Thus, we have

$$\frac{1}{2}\sum_{k=0}^{3} \sigma_k |\psi\rangle|A_k\rangle \to \frac{1}{2}\sum_{k=0}^{3} \sigma_k |\psi\rangle U_{23}|A_k\rangle = |\phi^+\rangle|\psi\rangle = |\Psi_{\mathrm{out}}\rangle. \tag{3}$$

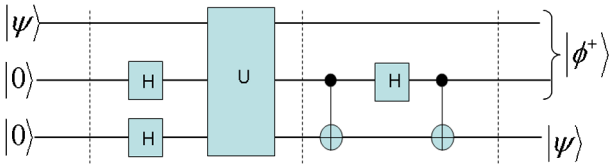

FIG. 1 (color online). Circuit diagram for testing the no-hiding theorem using the state randomization. U is the unitary operator for randomization and H represents the Hadamard gate. Dots and circles represent the CNOT gates. After randomization, the state $|\psi\rangle$ on the first qubit has been transferred to the ancilla qubit.

From (3) we can see that the first and the second qubits are in the Bell state and the third qubit contains the original information. Thus, the missing information can be fully recovered from the ancilla in intact form.

Liquid state nuclear magnetic resonance (NMR) has been successfully used as a test bed for a large number of quantum information protocols including Grover's algorithm [11], Shor's algorithm [12], quantum teleportation [13], adiabatic quantum computation [14,15], estimation of the ground state of hydrogen atom up to 45 bits [16], and more recently experimental verification of the nondestructive discrimination of Bell states [17]. Here, we report an experimental verification of the quantum no-hiding theorem using NMR. Experiments have been performed in a three qubit heteronuclear spin system formed by the ^{1}H, ^{19}F, and ^{13}C nuclei of ^{13}C-enriched dibromo fluoro methane ($^{13}CHFBr_2$) [18]. Figure 2(a) shows the equilibrium spectrum for the three nuclei at 300 K recorded in a Bruker AV500 spectrometer, where the resonance frequencies of ^{1}H, ^{19}F, and ^{13}C are 500, 470, and 125 MHz, respectively. We have taken ^{1}H, ^{19}F, and ^{13}C as the first, the second, and the third qubit, respectively.

Using the quantum circuit of Fig. 1, an equivalent NMR pulse sequence has been developed here (Fig. 3). This includes (i) the preparation of the pseudopure state (PPS) [18], (ii) the process of initialization, (iii) the randomization operation using its unitary extension, (iv) extraction of the original quantum information from the ancilla by applying local unitary transformations, and (v) finally, the measurement (reconstruction of density matrices via tomography). These sequence of steps can be represented by schematic use of several U_{ij} blocks (shown in light gray). During the application of U_{ij} the system evolves under the scalar coupling J_{ij} between the spins i and j for a time period of $1/2J_{ij}$. They create two spin order modes from a single spin transverse mode and vice versa. The π pulses in the center of U_{ij} are used to refocus all the chemical shifts and all the scalar couplings except between the spins i and j [18].

The experiment consists of implementing the above five steps on the three qubit system. The initial part of Fig. 3 contains preparation of $|000\rangle$ PPS by the spatial averaging method [19]. The initial state $|\psi\rangle_1|A\rangle_{23}$ [see (2)] is prepared from $|000\rangle$ PPS by applying a $(\theta)_\phi$ pulse on the first spin and $[\pi/2]_{-y}$ pulses (Hadamard gates) on the second and the third spins, respectively. The Hadamard

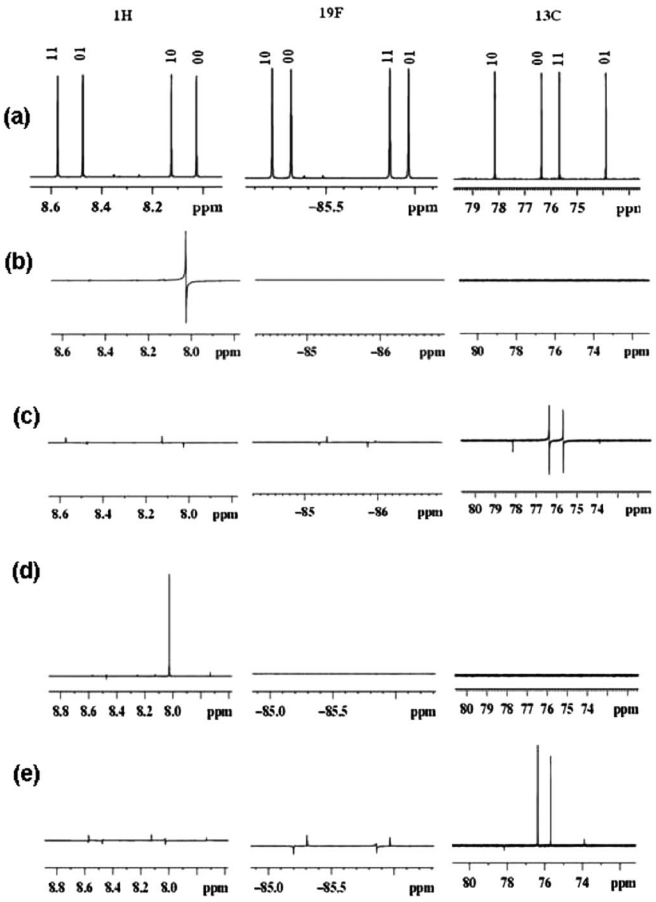

FIG. 2. (a) The equilibrium spectra of $^{13}CHFBr_2$ dissolved in acetone-d6 at 300 K on a AV500 NMR spectrometer. Labeling of the transition is given on top of each spectral line. The scalar couplings between different spins are measured as $J_{HC} = 224.5$, $J_{FC} = -310.9$, $J_{HF} = 49.7$. For $\theta = \pi/2$ and $\phi = 0$, (b) and (c) are, respectively, the experimental spectra for the input $(|\psi\rangle_1|00\rangle_{23})$ and output $(|\phi^+\rangle_{12}|\psi\rangle_3)$ state for the 3 spins. The receiver phase is set using a separate experiment so that y magnetization appears as positive absorption mode. For $\theta = \phi = \pi/2$, (d) and (e) are the experimental spectra showing, respectively, the input and output states for the 3 spins.

gate $[\pi/2]_{-y}$ on the second and third qubits transforms $|00\rangle$ to $|A\rangle$. Then, we need to perform the randomization operation U. Here, we have converted this into NMR pulse sequence by the use of a novel algorithmic technique for efficient decomposition of the unitary operators developed in our laboratory [20]. This method uses graphs of a complete set of base operators and develops an algorithmic technique for finding the decomposition of a given unitary operator into basis operators and their equivalent pulse sequences. Thus, U can be expressed as $U = \exp(-i\frac{\pi}{4}\mathbf{1})\exp(i\frac{\pi}{2}I_{3z})\exp(-i\pi I_{1y}I_{2z})\exp(-i\pi I_{1z}I_{3z})\exp(i\frac{\pi}{2}I_{1x})\exp(i\frac{\pi}{2}I_{1z})$. The first term yields only an overall phase and can be neglected. The second and last terms are $\pi/2$ rotations of the third and the first qubits, respectively, about the z axis. The z rotation is achieved by the composite pulse $[\pi/2]^i_{-z} = [\pi/2]^i_x[\pi/2]^i_{-y}[\pi/2]^i_{-x}$, where i $(i = 1, 2, 3)$

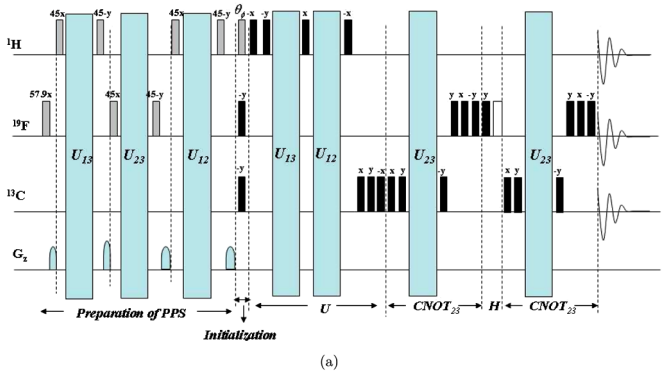

FIG. 3 (color online). NMR pulse sequence for the implementation of the no-hiding theorem. The filled and the empty boxes, respectively, represent $\pi/2$ and π pulses while the gray boxes represent pulses with flip angles on the top. The phase of a pulse is given on top of the pulse for $\pi/2$ and π pulses and are subscripts of angles for other flip angle pulses. G_z is the z-gradient pulse used to destroy all unwanted transverse magnetization. For each (θ, ϕ) pair three identical experiments are performed to observe each qubit independently.

refers to various qubits. The fourth term is U_{13} and the third term can be converted to U_{12} by converting I_{1y} to I_{1z} using the pulse $[\pi/2]_{-x}[\pi/2]_y[\pi/2]_x$. The final pulse sequence is obtained as $[\pi/2]^3_{-z}[\pi/2]^1_{-x}U_{12}[\pi/2]^1_x U_{13}[\pi/2]^1_{-x} \times [\pi/2]^1_{-z}$. Here, pulses are always applied from right to left.

The next step is extraction of quantum information $|\psi\rangle$ from the ancilla qubits. As we have seen, this can be achieved by applying two CNOT gates and one Hadamard gate (Figs. 1 and 3). The CNOT$_{23}$ gate in NMR is realized by the following pulse sequence [21]: $[\pi/2]^2_{-y}[\pi/2]^2_x \times [\pi/2]^2_y[\pi/2]^3_{-y}U_{23}[\pi/2]^3_y[\pi/2]^3_x$. Finally, we need to do measurements to confirm our result. All the qubits are directly observed at the end of the computation and no measuring pulse is required. The missing information about $|\psi\rangle$ is actually found in the state of the third qubit. This requires taking the trace over the first and the second qubits. One of the ways of taking this trace is to decouple the first and the second qubits while observing the third qubit [22]. However, this leads to excessive sample heating [22]. We have therefore performed the trace numerically by measuring all the three qubits and appropriately adding the signal intensities [23].

If we write the full density matrix of the output state $|\Psi_{\text{out}}\rangle$ (with the states ordered as 000, 001, 010, 011, 100, 101, 110, 111), then we will see that this contains two single quantum terms of amplitude $\alpha\beta^*$ on the third qubit [σ_{12}, σ_{78}, and complex conjugate (CC)] which are directly observable. Since both the single quantum coherences of the third spin are represented by $\alpha\beta^*$, they are in phase with each other. We note that no single quantum coherence of spins 1 and 2 are present as they are in the Bell state. There are two double quantum terms of amplitude α^2 and β^2 (σ_{17} and σ_{28} and CC) and one triple quantum term of amplitude $\alpha\beta^*$ (σ_{18} and CC) which are not directly observable. They have been observed (for tomography) by converting them to observable single quantum term [24].

The results are summarized in Figs. 2 and 4. We have measured a total of 325 input states arranged on a 13×25 rectangular grid of $\theta(0 \rightarrow \pi)$ and $\phi(0 \rightarrow 2\pi)$ values with a

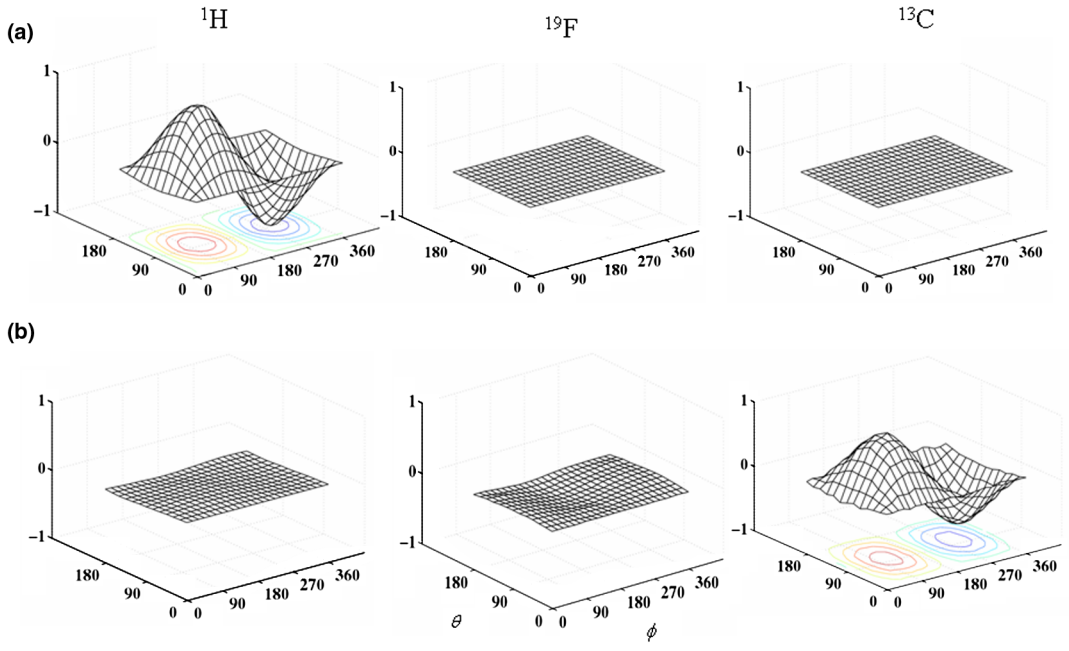

FIG. 4 (color online). Summarized experimental results for the no-hiding theorem using the state randomization. The integrals of the real part of the NMR signal from spins ^{1}H, ^{19}F, and ^{13}C are shown as mesh and contour plots as a function of θ and ϕ. The plots show the expected sine and cosine behavior. (a) Input state $|\psi\rangle_1|00\rangle_{23}$. The information about θ and ϕ is encoded in the first spin, and second and third spins are in $|00\rangle$ state. (b) Quantum information has been transferred from the first qubit to the third qubit.

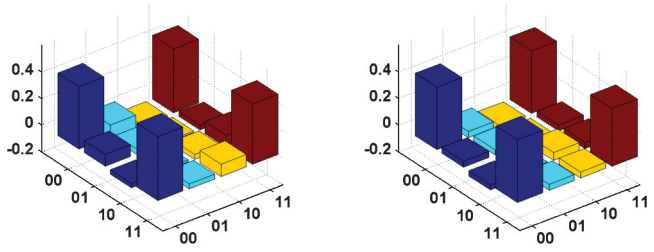

FIG. 5 (color). The output density matrix for the first two qubits showing that they are in the Bell state $|\phi^+\rangle$. (a) $\theta = \phi = \pi/2$. (b) $\theta = \pi/2$ and $\phi = \pi$.

spacing of 15^0. The experimental spectra of the input and output states for $\theta = \pi/2$, $\phi = 0$ are, respectively, given in Figs. 2(b) and 2(c). Similarly, for $\theta = \phi = \pi/2$ these are, respectively, given in Figs. 2(d) and 2(e). The receiver phase is set such that we get positive absorption lines for the input state $\theta = \phi = \pi/2$. For each input state we have separately measured the total NMR signal (integration of the entire multiplet) observed from all the spins 1, 2, and 3, and their real components are plotted in Fig. 4. Figure 4(a) shows the input state $|\psi\rangle_1|00\rangle_{23}$ and Fig. 4(b) shows the output state $|\phi^+\rangle_{12}|\psi\rangle_3$. The experimental results (Fig. 4) clearly show the modulation of the expected lines, thus showing the coherent quantum oscillations of the original qubit. This ensures that quantum information which has disappeared from the first qubit actually resides in the third qubit in accordance with the no-hiding theorem.

Additionally, we have reconstructed the density matrices of the output state for several values of θ and ϕ by quantum state tomography [24]. The density matrix of the output state for $\theta = \phi = \pi/2$ has been plotted (figure not shown). The experimental state tomography confirms the theoretical output state as desired. The fidelity of the measurement has been evaluated for several values of θ and ϕ using the parameters "average absolute deviation $\langle \Delta X \rangle$" and the "maximum absolute deviation $\Delta X_{\max}$" as defined by $\langle \Delta X \rangle = \frac{1}{N^2} \sum_{i,j=1}^{N} |x_{i,j}^T - x_{i,j}^E|$, and $\Delta X_{\max} = \max|x_{i,j}^T - x_{i,j}^E| \;\; \forall \; i, j \in \{1, N\}$, where $x_{i,j}^T$, $x_{i,j}^E$ are the theoretical and the experimental elements [18]. The average absolute deviation (for three θ and ϕ values) $\langle \Delta X \rangle$ was found to be $\sim 2\%$ and the maximum absolute deviation $\Delta X_{\max}$ was found to be $\sim 5\%$.

In our experiment the reduced density matrices of the first two qubits of the output states ($|\phi^+\rangle$ of Fig. 1) have also been tomographed to observe the fidelity of the Bell states in the first two qubits at the end of the measurement. Figure 5 contains the Bell state $|\phi^+\rangle_{12}$ for the input state with parameters (a) $\theta = \phi = \pi/2$ and (b) $\theta = \pi/2$, $\phi = 0$. Figure 5 confirms that the first two qubits remain in the Bell state irrespective of the changes in (θ, ϕ), and the original information about (θ, ϕ) has been transferred to the third qubit. The average absolute deviation $\langle \Delta X \rangle$ was found to be $\sim 5\%$ and the maximum absolute deviation $\Delta X_{\max}$ was found to be $\sim 7\%$. The experimental errors can originate from rf inhomogeneities, imperfect calibration of rf pulses, and decoherence. However, in the present experiment the decoherence errors are likely to be small, since the total experimental time (Fig. 3) is ~ 30 msec while the shortest T_2 (of ^{19}F) of the sample is 700 msec.

To conclude, we have performed a proof-of-principle demonstration of the no-hiding theorem and addressed the question of missing information on a 3-qubit NMR quantum information processor. Using the state randomization as a prime example of the bleaching process, we have found that the original quantum information which is missing from the first qubit indeed can be recovered from the ancilla qubits. No information is found to be hidden in the bipartite correlations between the original qubit and the ancilla qubits. To the best of our knowledge, this is the first experimental verification of a fundamental theorem of quantum mechanics.

We thank P. Rungta and S. L. Braunstein for useful discussions.

*Deceased.
[1] W. K. Wootters and W. H. Zurek, Nature (London) **299**, 802 (1982).
[2] A. K. Pati and S. L. Braunstein, Nature (London) **404**, 164 (2000).
[3] R. Jozsa, IBM J. Res. Dev. **48**, 79 (2004).
[4] M. Horodecki *et al.*, Found. Phys. **35**, 2041 (2005).
[5] S. L. Braunstein and A. K. Pati, Phys. Rev. Lett. **98**, 080502 (2007).
[6] S. L. Braunstein, Phys. Rev. A **53**, 1900 (1996).
[7] S. L. Braunstein, H. K. Lo, T. Spiller (unpublished).
[8] M. Mosca, A. Tapp, and R. Wolf, arXiv:quant-ph/0003101.
[9] S. W. Hawking, Nature (London) **248**, 30 (1974).
[10] R. Landauer, IBM J. Res. Dev. **5**, 183 (1961).
[11] I. L. Chuang, N. Gershenfeld, and M. Kubinec, Phys. Rev. Lett. **80**, 3408 (1998).
[12] L. M. K. Vandersypen *et al.*, Nature (London) **414**, 883 (2001).
[13] M. A. Nielsen *et al.*, Nature (London) **396**, 52 (1998).
[14] A. Mitra *et al.*, J. Magn. Reson. **177**, 285 (2005).
[15] X. Peng *et al.*, Phys. Rev. Lett. **101**, 220405 (2008).
[16] J. Du *et al.*, Phys. Rev. Lett. **104**, 030502 (2010).
[17] J. R. Samal *et al.*, J. Phys. B **43**, 095508 (2010).
[18] A. Mitra *et al.*, J. Magn. Reson. **187**, 306 (2007).
[19] D. G. Cory *et al.*, Proc. Natl. Acad. Sci. U.S.A. **94**, 1634 (1997).
[20] A. Ajoy *et al.* (to be published).
[21] A. M. Childs, I. L. Chuang, and D. W. Leung, Phys. Rev. A **64**, 012314 (2001).
[22] Y. Sharf *et al.*, Mol. Phys. **98**, 1347 (2000).
[23] H. K. Cummins *et al.*, Phys. Rev. Lett. **88**, 187901 (2002).
[24] A. Mitra and A. Kumar, J. Indian Inst. Sci. **89**, 309 (2009).